extract of sample A, respectively, in the presence of S9 mix. Although the values of MI indicated no cytotoxicity, the ratio of live cells to total cells on the preparation was around 50% and 10%, respectively. Actually a few remaining live cells on the preparation of 40% extract of sample A were well and the chromosome morphology of the metaphase cells was fine.

Numerical chromosome aberrations consist of polyploidy and aneuploidy. Aneuploidy has been implicated in sterility, abortions, stillbirths, congenital abnormalities, and carcinogenesis.[22,23] The *in vitro* CA test is not routinely used to detect aneuploidy, although it could be,[24] but polyploid induction suggests the possibility of aneuploid induction. In the present study, sample A, which had a high concentration of MBT, induced a high frequency of polyploidy in the presence of S9 mix. MBT alone at the same concentration also induced polyploidy, but with a lower frequency and with accompanying endoreduplication. Thus, the induction of polyploidy by sample A did not seemed to be explained simply by the presence of MBT.

Endoreduplication, which shows an characteristic morphology (diplochromosomes), is an endomitotic chromosome duplication that occurs without mitosis-like events during interphase.[25] A typical endoreduplication event is characterized by two periods of DNA synthesis, S1 and S2, separated by a G period of variable duration.[26] Some chemicals, such as 4NQO, acridine yellow, cytoxan, captan,[27] and rotenone,[28] induce endoreduplication without S9 mix. The frequency of endoreduplication induced by those compounds was similar to the frequency induced by MBT in the present study.

The fact that sample A showed stronger cytotoxicity and induced a higher frequency of polyploidy than was predicted by MBT alone might have been due to the presence of other leachables in the sample. This suggests that sample A may be useful as a positive control for the safety evaluation of biomaterials and that the test might overcome the poor predictive value of individual components of materials.

In the Japanese guidelines for basic biological tests of medical materials and devices, the use of V79 cells is preferred in the cytotoxicity test. In the test the introduction of a metabolic activation system is not required. On the other hand, genotoxicity tests require the use of an exogenous metabolic activation system and of their methods following Japanese guidelines for drugs and chemicals, and OECD guidelines. CHL cells are popular in the CA test in Japan. In the present study each of the cytotoxicity test and the CA test followed the corresponding guideline independently. The difference in the cytotoxicty of sample A between with and without S9 mix suggests that the discussion of the introduction of an exogenous metabolic activation system into the cytotoxicity test may be needed.

References

1. MHW Notification YAKUKI No 99 (1995. 6. 27). Guidelines for basic biological tests of medical materials and devices.
2. Ikarashi Y, Toyoda K, Ohsawa N, Uchima T, Tsuchiya T, Kaniwa M, Sato M, Takahashi M, Nakamura A. Comparative studies by cell culture and in vivo implantation test on the toxicity of natural rubber latex materials. J Biomed Mater Res 1992;26:339–356.
3. Crippa M, Belleri L, Mistrello G, Carsana T, Neri G, Alessio L. Prevention of latex allergy among health care workers: evaluation of the extractable latex protein content in different types of medical gloves. Am J Ind Med 2003;44:24–31.
4. Yip ES. Accommodating latex allergy concerns in surgical settings. AORN J 2003;78:595–598, 601–603.
5. Acero S, Alvarez MJ, Garcia BE, Echechipia S, Olaguibel JM, Tabar AI. Occupational asthma from natural rubber latex. Specific inhalation challenge test and evolution. J Invest Allergol Clin Immunol 2003;13:155–161.
6. Ruutu M, Alfthan O, Heikkinen L, Järvinen A, Lehtonen T, Merikallio E, Standertskjöld-Nordenstam CG. "Epidemic" of acute urethral stricture after open-heart surgery. Lancet 1982; 1:218.
7. Smith JM, Neligan M. Urethral strictures after open heart surgery [letter]. Lancet 1982;1:392.
8. Fraser ID, Beaton NR, McGinn EP. Catheters and postoperative urethral stricture [letter]. Lancet 1982;1:622.
9. Syme RR. Epidemic of acute urethral stricture after prostate surgery. Lancet 1982;2:925.
10. Ruutu M, Alfthan O, Heikkinen L, Järvinen A, Konttinen M, Lehtonen T, Merikallio E, Standertskjöld-Nordenstam CG. Unexpected urethral strictures after short-term catheterization in open-heart surgery. Scand J Urol Nephrol 1984;18:9–12.
11. Nakamura A, Kanazawa Y, Sato H, Tsuchiya T, Ikarashi T, De Jong WH, Andersen KE, Knudsen B. Evaluation of allergic potential of rubber products: comparison of sample preparation methods for the testing of polymeric medical devices. J Toxicol 2003;22:169–185.
12. Elkind MM, Sutton H. Radiation response of mammalian cells grown in culture, I. Repair of X-ray damage in surviving Chinese hamster cells. Radiat Res 1960;13:556–593.
13. Koyama H, Utakoji T, Ono T. A new cell line derived from newborn Chinese hamster lung tissue. Gann 1970;61:161–167.
14. Ishidate M Jr, Odashima S. Chromosome tests with 134 compounds on Chinese hamster cells in vitro – a screening for chemical carcinogens. Mutat Res 1977;48:337–354.
15. Matsuoka A, Hayashi M, Ishidate M Jr. Chromosomal aberration tests on 29 chemicals combined with S9 mix in vitro. Mutat Res 1979;66:277–290.
16. Matsuoka A, Sofuni T, Miyata N, Ishidate M Jr. Clastogenicity of 1-nitropyrene, fluorene, and mononitrofluorenes in cultured Chinese hamster cells. Mutat Res 1991;259:103–110.
17. Nakamura A, Ikarashi Y, Tsuchiya T, Kaniwa MA, Sato M, Toyoda K, Takahashi M, Ohsawa N, Uchima T. Correlations among chemical constituents, cytotoxicities and tissue responses: in the case of natural rubber latex materials. Biomaterials 1990;11:92–94.
18. Tinkler J, Gott D, Bootman J. Risk assessment of dithiocarbamate accelerator residues in latex-based medical devices: genotoxicity considerations. Food Chem Toxicol 1998;36:849–866.
19. Hedenstedt A, Rannug U, Ramel C, Wachtmeister CA. Mutagenicity and metabolism studies on 12 thiuram and dithiocarbamate compounds used as accelerators in the Swedish rubber industry. Mutat Res 1979;68:313–325.
20. Rannug A, Rannug U, Ramel C. Genotoxic effects of additives in synthetic elastomers with special consideration to the mechanism of action of thiurams and dithiocarbamates. Prog Clin Biol Res 1984;141:407–419.

21. Anderson BE, Zeiger E, Shelby MD, Resnick MA, Gulati DK, Ivett JL, Loveday KS. Chromosome aberration and sister chromatid exchange test results with 42 chemicals. Environ Mol Mutagen 1990;16(suppl 18):55–137.
22. Barrett JC, Oshimura M, Tanaka N, Tsutsui T. Role of aneuploidy in early and late stage of neoplastic progression of Syrian hamster embryo cells in culture. In: Holllaender A, editor. Aneuploidy-etiology and mechanisms. New York: Plenum Press; 1985. p 523–538.
23. Oshimura M, Barrett JC. Chemically induced aneuploidy in mammalian cells: mechanisms and biological significance in cancer. Environ Mutagen 1986;8:129–159.
24. Matsuoka A, Ozaki M, Takeshita K, Sakamoto H, Glatt HR, Hayashi M, Sofuni T. Aneuploidy induction by benzo[a]pyrene and polyploidy induction by 7,12-dimethylbenz [a]anthracene in Chinese hamster cell lines V79-MZ and V79. Mutagenesis 1997;12:365–372.
25. Levan A, Hauschka TS. Endomitotic reduplication mechanisms in ascites tumors of the mouse. J Natl Cancer Inst 1953; 14:1–43.
26. Rizzoni M, Palitti F. Regulatory mechanism of cell division, I. Colchicine-induced endoreduplication. Exp Cell Res1973;77:450–458.
27. Sutou S, Tokuyama F. Induction of endoreduplication in cultured mammalian cells by some chemical mutagens. Cancer Res 1974;34:2615–2623.
28. Matsumoto K, Ohta T. Rotenone induces aneuploidy, polyploidy and endoreduplication in cultured Chinese hamster cells. Mutat Res 1991;263:173–177.

ELSEVIER

Chemosphere 60 (2005) 1279–1287

CHEMOSPHERE

www.elsevier.com/locate/chemosphere

Monitoring of polycyclic aromatic hydrocarbons and water-extractable phenols in creosotes and creosote-treated woods made and procurable in Japan

Yoshiaki Ikarashi *, Masa-aki Kaniwa, Toshie Tsuchiya

National Institute of Health Sciences, Division of Medical Devices, 1-18-1, Kamiyoga, Setagaya-ku, Tokyo 158-8501, Japan

Received 2 July 2004; received in revised form 21 December 2004; accepted 18 January 2005
Available online 2 March 2005

Abstract

The recycling of disused railway sleepers treated with wood preservatives such as creosote as exterior wood for use in gardens has recently become popular in Japan. Creosote contains high quantities of polycyclic aromatic hydrocarbons (PAHs), and can lead to skin irritation and disease. In this work we have determined the amount of PAHs and water-extractable phenols in creosote and creosote-treated wood products such as railway sleepers and stakes for agricultural use that are either made or are procurable in Japan. PAHs were extracted with dichloromethane and analyzed by gas chromatography–mass spectrometry. Among carcinogenic PAHs, benz(*a*)anthracene was detected in the highest concentration, varying between 228 and 6328 μg/g in creosotes. Benzo(*b*)fluoranthene, benzo(*k*)fluoranthene and benzo(*a*)-pyrene (BaP) were found in the range of 67–3541 μg/g. Almost all creosotes contained more than 50 μg/g of BaP, which is the upper limit level that is permitted in the European Union (EU). Creosote-impregnated wood products, such as brand-new or secondhand railway sleepers and foundations, contained large amounts of BaP (58–749 μg/g) and benz(*a*)anthracene (250–1282 μg/g). Concentrations of between 692 and 2489 μg/g of phenols were determined in the water extracts from creosotes, but the level was considerably less than the EU control value (3% by mass), and there was no correlation between the amount of water-extractable phenols and the amount of PAHs detected in each sample. The situation that consumers are free to use the creosotes containing a high concentration of carcinogens such as BaP may cause unacceptable damage to the health of persons handling these creosote products.

Keywords: Polycyclic aromatic hydrocarbons; Creosote; GC–MS; Phenols; Wood preservative

1. Introduction

Creosote is a mid-heavy distillate of coal tar with a boiling point of between 200 and 400 °C (Gevao and Jones, 1998). The annual production of creosote in Japan is about 70 million tons. The majority of this is used as raw material for carbon black, while much of the rest has been used as a wood preservative (market research of Journal of The Japan Aromatic Industry Association, Inc. and Japan Wood Preserving Association). Wood treated with creosote was formerly used for railway sleepers and poles for the transport of electricity. These items are now commonly used in the foundations

* Corresponding author. Tel.: +81 3 3700 1141; fax: +81 3 3707 6950.
E-mail address: ikarashi@nihs.go.jp (Y. Ikarashi).

0045-6535/$ - see front matter © 2005 Elsevier Ltd. All rights reserved.
doi:10.1016/j.chemosphere.2005.01.054

20×, 100×, 500× and 1000×) was prepared. Two millilitres of each (diluted) extraction solution was spiked with 0.5 ml of the internal standard solution (e.g. acenaphthene-d10 20 μg in dichloromethane) and the sample solution (1 μl) was injected into the GC–MS system. The desorption time was 60 s in split-less mode. The GC column temperature was programmed as follows; it was first maintained at 60 °C for 3 min and was then heated at a rate of 10 °C/min up to 300 °C, after which it was held at this temperature for 5 min. The injection temperature was maintained at 280 °C. The GC–MS transfer line temperature was 280 °C and the ion source temperature was 180 °C. The carrier gas was helium and column flow was maintained at 1.0 ml/min. The MS electron impact ionization energy was 70 eV. Detection was carried out using full scan (TIC, $m/z = 45$–500) and selective ion monitoring (SIM). Compounds in the sample solutions were identified from their retention times and from agreement with the mass chromatograms of the PAH standard solutions using a Bench-Top/PBM Mass Spectral Identification (Palisade Co., USA) with the Wiley Registry of Mass Spectral Data (John Wiley & Sons. Inc., USA). The PAH standard solutions (e.g. 0.5, 1, 2, 5 and 10 μg/ml) spiked with 0.5 ml of the internal standard solution were injected into the system and the calibration curves for the ratio of the peak area of each PAH to the internal standard for the respective mass of each ion was established. Each PAH concentration (μg/ml) in an appropriate diluted sample solution was derived from the calibration curves, and then the contents of PAHs (μg) per 1 g of sample were derived.

2.5. Analysis of water extractable phenols

2.5.1. Extraction

A creosote oil sample (0.1 ml) was shaken with 5 ml of water for 30 min, and a water layer containing the water-extractable phenols was obtained by centrifuging at 3000 rpm for 5 min.

For wood products, the following extraction conditions were used. Condition 1: About 1.0 g of the sample was cut into small pieces (described above) and was weighed into a 50 ml glass bottle and 10 ml of water was added. The bottle was stopped tightly and autoclaved at 121 °C for 15 min. Condition 2: The sample (1.0 g) and 10 ml of water were put into a glass bottle, shaken at room temperature for 1 h and heated at 37 °C for 24 h. The extract was obtained by filtration.

2.5.2. Determination

The content of the water-soluble phenols was determined by the 4-aminoantipyrin method (Pharmaceutical Society of Japan, 2000). The extract was reacted with 4-aminoantipyrin and potassium ferricyanide in boric acid buffer, and the absorbance of the solution was measured at a wavelength of 510 nm. The phenol concentrations in 1 g of the samples were derived from the calibration curve.

3. Results and discussion

3.1. PAH in creosote

Column chromatography is generally used to extract PAHs from the various chemicals in creosote (Rotard and Mailahn, 1987; Shu et al., 2003; Ou et al., 2004). In this study, we separated the target PAHs by a solid phase extraction approach using Sep-Pak Plus silica-cartridges. Creosote (0.1 ml) was loaded on a Sep-Pak silica cartridge and eluted with 10 ml of dichloromethane. The concentrations of the PAHs in each fraction were determined and compared with those in the original creosote that had not been cleaned up. Each PAH was recovered at high yield (97–133%, data not shown). After washing with dichloromethane, a black-colored layer still remained at the top of the cartridge that could have contaminated the GC column and MS detector. The main object of the solid extraction was to remove these contaminants.

The analysis results for the nine creosotes and the three oil-based wood preservative paints are shown in Table 2. The limit of quantification (LOQ) of each PAH in the sample (not determined, ND) was estimated as about 40 μg/g, which was calculated from the lowest concentration (0.2 μg/ml) that can be determined in the diluted sample solution injected into the GC–MS. Among the 16 PAHs that we monitored, naphthalene, acenaphthene, fluorene, phenanthrene and anthracene were detected in high concentrations in commercially-available creosote samples. Of the carcinogenic PAHs that were classified as cancer risk 2A or 2B (IARC, 1983), benz(*a*)anthracene was detected in the highest concentration, varying between 228 and 6328 μg/g. Isomers of benzofluoranthenes and BaP were detected at similar levels in the range of 67–3541 μg/g. The amounts of indeno(1,2,3-*cd*)pyrene, dibenz(*a,h*)anthracene and benzo(*ghi*)perylene were ND–599 μg/g, ND–122 μg/g and ND–620 μg/g, respectively. In contrast, the constituents of the wood preservative paints (not creosote) were completely different, and these did not contain four- to six-ring PAHs above the LOQ. The PAH profiles (constituents and levels) of creosotes commercially-available in Japan were similar to those of the old type of creosotes used in Europe (Woolgar and Jones, 1999; Kohler et al., 2000). Since 1994, improved creosotes have been used for wooden railroad ties in Switzerland, and these contain BaP at levels below 50 μg/g by fractionating lower boiling components to reduce the amounts of carcinogenic four- to six-ring PAHs (Kohler et al., 2000). Among the creosote samples that

Table 2
PAH content in creosotes and non-creosote type wood preservative paints

Chemical	PAH content (μg/g)											
	Creosote									Wood preservative (non-creosote)		
	A	B	C	D	E	F	G	H	I	NA	NB	NC
Naphthalene	21349	24648	42174	54866	29462	13777	58857	25333	22261	423	31856	52031
Acenaphthylene	4785	3186	1961	2261	1852	1895	7950	1480	2035	ND	ND	ND
Acenaphthene	30899	26737	55628	69622	50065	55360	84230	80764	55143	ND	ND	ND
Fluorene	30868	27547	17081	20627	25433	35433	83857	14462	30119	41	ND	ND
Phenanthrene	27646	21059	55480	64249	90127	33830	13434	45240	113846	ND	ND	ND
Anthracene	9771	7168	18391	15110	15489	8905	4751	11954	14220	ND	ND	ND
Fluoranthene	9946	4292	23251	19766	28001	5221	589	25819	31856	ND	ND	ND
Pyrene	5429	2240	12695	10323	15787	3410	220	17964	16763	ND	ND	ND
Benz(*a*)anthracene	228	3637	2494	1706	3859	5616	ND	6328	4795	ND	ND	ND
Chrysene	170	3035	1875	1454	3299	4033	ND	7153	4067	ND	ND	ND
Benzo(*b*)fluoranthene	91	506	216	172	692	1183	ND	3541	664	ND	ND	ND
Benzo(*k*)fluoranthene	79	358	165	132	468	876	ND	1532	449	ND	ND	ND
Benzo(*a*)pyrene	67	260	116	108	465	882	ND	2514	433	ND	ND	ND
Indeno(1,2,3-*cd*)pyrene	ND	ND	ND	ND	57	105	ND	599	ND	ND	ND	ND
Dibenz(*a,h*)anthracene	51	ND	ND	ND	ND	ND	ND	122	ND	ND	ND	ND
Benzo(*ghi*)perylene	ND	ND	ND	ND	ND	69	ND	620	ND	ND	ND	ND

ND was < 40 μg/g.

we tested, only sample G contained BaP at less than 50 μg/g. According to the manufacturer, this sample was produced for export to the EU. From these results, it became clear that creosote containing a high concentration of BaP is still sold and that the general public is still free to use such creosote for wood preservation in Japan. This situation may cause impermissible health damage to persons treating wood with these creosote products. The quality of creosote that may be used as a wood preservative under the Japanese Industrial Standard (JIS, 2004) has been revised.

3.2. PAH in creosote-treated wood

Several solvents were used for the extraction of PAHs from creosote-treated woods. In our limited experiment, dichloromethane showed higher extraction efficiency than hexane, ethanol and methanol (data not shown). In addition, the dichloromethane-extract was loaded directly into the Sep-Pak silica cartridges and eluted with the solvent to prepare the sample solutions. Therefore, we found that dichloromethane was a suitable extraction solvent for PAHs from creosote-treated wood.

We examined whether soak extraction using dichloromethane could be used as an alternative to Soxhlet extraction. In the soak extraction, 1 g of creosote-treated wood was incubated in 10 ml of dichloromethane. In the Soxhlet-extraction method, 5.0 g of the sample was extracted with 100 ml of dichloromethane at 50 °C for 24 h. The concentrations of the 13 PAHs extracted from samples of creosote-treated wood under both sets of conditions are shown in Table 3. These show that similar levels of PAHs can be released by both dichloromethane soak extraction and by Soxhlet extraction. Although Schwab et al. (1999) stated that Soxhlet extraction has some potential for the loss of volatile compounds, such decrease in naphthalene, el al. was not observed in this study. However, the Soxhlet extraction technique requires special apparatus and long extraction periods. There was not a significant difference between soak extraction at room temperature and at 37 °C over a 24 h period, but the total amounts extracted for 24 h incubation were higher than those were achieved by shake extraction for 1 h. Therefore, in this study, creosote-treated wood was soaked in dichloromethane at 37 °C for 24 h and the amount of PAH in the extract was measured.

Sections taken approximately 3 cm in depth from the surface of the wood samples (railway sleepers, foundations, stakes) were extracted and the amount of PAHs was determined (Table 4). The LOQ of PAH in wood sample was about 4 μg/g, which was derived as described above. In the brand-new creosote-treated products, the foundation (sample 1) and the railway sleepers (samples 2 and 3), phenanthrene were found to have the highest concentrations, and elevated amounts of acenaphthene, fluorene, anthracene and fluoranthene were also detected. The concentration of five- and six-ring PAHs in the used railway sleeper (sample 5) was higher than that in the new products. The level of BaP in foundations and in railway sleepers was 58–749 μg/g, while for benz(*a*)anthracene it was 250–1282 μg/g. Only small amounts of these compounds were detected in the untreated railway sleepers (sample 6). These results

Table 3
Effect of extraction condition on the recovery of PAH from creosote-treated wood samples

Chemical	Found (μg/g)			
	Shake (rt, 1 h)	Stand (rt, 24 h)	Stand (37 °C, 24 h)	Soxhlet-extraction (50 °C, 24 h)
Naphthalene	83	176	295	383
Acenaphthylene	85	114	173	158
Acenaphthene	2811	4388	4854	5740
Fluorene	3305	4178	4385	5090
Phenanthrene	11841	17020	17578	12620
Anthracene	4249	5150	4728	4790
Fluoranthene	4536	5900	6406	5590
Pyrene	3577	4360	4494	4740
Benz(*a*)anthracene	1013	1104	1019	989
Chrysene	987	1067	976	939
Benzo(*b*)fluoranthene	327	471	558	377
Benzo(*k*)fluoranthene	238	286	382	309
Benzo(*a*)pyrene	206	267	380	280

rt = room temperature.
Creosote-treated wood was cut in small pieces and 1.0 g was weighed into a tube. Dichloromethane 10 ml was added and the sample was extracted using each of the conditions listed. In the Soxhlet-extraction, 5.0 g of the sample was extracted with 100 ml of dichloromethane at 50 °C for 24 h. The eluate was taken by filtration and 1 ml of the eluate was loaded on a Sep-Pak silica cartridge and eluted with 10 ml dichloromethane. The eluate was adjusted to an appropriate volume with dichloromethane and injected into the GC–MS. The concentration of PAH in the sample was measured.

Table 4
Content of PAHs in wood products

Chemical	Amount (μg/g)							
	1	2	3	4	5	6	7	8
Naphthalene	374	1017	1064	439	338	7	303	6
Acenaphthylene	212	290	245	197	232	4	187	4
Acenaphthene	2000	4251	8043	2355	449	ND	266	4
Fluorene	1764	3131	2754	3207	390	ND	101	ND
Phenanthrene	6040	6069	1270	10619	7837	ND	105	ND
Anthracene	1831	1026	915	2573	1124	4	33	5
Fluoranthene	2447	1144	843	6013	7966	ND	24	ND
Pyrene	1411	813	731	3702	7278	ND	14	ND
Benz(*a*)anthracene	787	250	336	1282	1058	ND	ND	ND
Chrysene	715	226	401	875	1094	ND	ND	ND
Benzo(*b*)fluoranthene	256	88	192	194	973	ND	ND	ND
Benzo(*k*)fluoranthene	157	62	94	154	601	ND	ND	ND
Benzo(*a*)pyrene	134	58	130	125	749	ND	ND	ND
Indeno(1,2,3-*cd*)pyrene	14	ND	58	13	323	ND	ND	ND
Dibenz(*a,h*)anthracene	ND	ND	7	ND	35	ND	ND	ND
Benzo(*ghi*)perylene	8	ND	54	9	288	ND	ND	ND

ND means < 4 μg/g.

suggested that the PAHs detected were derived from the treatment with creosote. We guess that the difference in the PAH content in the samples was caused by the difference in the manufacturing method of creosote and the impregnation amount of creosote into the woods.

Kohler et al. (2000) reported that naphthalene and acenaphthene in the top layer of railroad ties had leached into the environment with aging, and carcinogenic compounds such as benz(*a,h*)anthracene and BaP etc. remained at the same level in the products over an extended time, so the relative concentrations of these chemicals were significantly higher in the top layer than in the inner layers. It suggested that the determination of the PAH content in the outer layers is important for assessing the risk to human health following skin contact with creosote-treated products. The creosote con-

tent in the railway sleepers and foundations those are creosote-impregnated wood products is not significantly different between the outer layers and the center layers. In contrast, the amount of PAHs in a stake sample (No. 7) is small. Macroscopic studies of sections taken 1–2 mm from the surface showed a change in color, so creosote does not penetrate into the center of the wood but remains near to the surface. Accordingly, almost all of a layer cut approximately 3 cm in depth from the surface of a stake does not contain any creosote, and the total creosote content was low when a test solution was prepared. In a preliminary experiment, the dissipation pattern of PAHs in an extract prepared from a section taken 2 mm in depth from the surface of a stake was comparable to that observed in the extract from a railway sleeper or from the liquid creosote used in this study. It is believed that the creosote used to treat the stake was not a special grade product with decreased four- to six-ring PAH content. No significant occurrences of skin cancer have been reported in workers in creosote-impregnation plants or in consumers, but CSTEE (1999) warned of the cancer risk from creosote containing 50 μg/g BaP and from wood treated with such creosote.

3.3. Water-extractable phenols in creosote

The difference of phenols amount extracted from creosote by increased shaking time from 10 min to 2 h was small. In this study, a creosote sample was shaken with water for 30 min at room temperature, and the water layer was obtained by centrifuging. Table 5 presents the content of water-extractable phenols in creosote and wood preservative paints. Typical phenol concentrations of between 692 and 2489 μg/g were found in creosotes. In contrast, lower concentrations of phenols were found in non-creosote-type wood preservatives. There was no correlation between the amount of water-extractable phenols and the amount of PAHs in each sample. The levels of phenols determined in these creosotes were considerably lower than the maximum levels permitted in the EU (3% by mass) and were similar to the data (between 0.06% and 0.77%) reported by Kohler et al. (2000). Creosotes that are commercially available in Japan receive an alkaline treatment after distillation (personal communication from a manufacturer), so the content of phenols is believed to be low.

Table 5
Content of water-extractable phenols in creosotes and non-creosote type wood preservatives

Sample		Water-extractable phenols (μg/g)
Creosote	A	1093
	B	1415
	C	692
	D	782
	E	2121
	F	2155
	G	1294
	H	2359
	I	2489
Wood preservative (non creosote)	NA	378
	NB	31
	NC	ND

The sample (0.1 g) was shaken with 5 ml water for 30 min and the water layer was obtained by centrifuging at 3000 rpm for 5 min. The content of water-extractable phenols was determined by the 4-aminoantipyrin method.

3.4. Water-extractable phenols in creosote-treated wood

There are a few reports on the investigation of water-extractable phenols in creosote-treated wood samples. In our preliminary examination, the detected phenol content increased with increasing extraction time and temperature. This means that migration of water into the sample for the extraction of phenols trapped inside the wood took a long time, and the quantity of water-extractable phenols detected varied with the extraction temperature and the incubation period.

Samples were extracted by autoclaving or incubation for 24 h at 37 °C. For all samples, the values obtained with the autoclave extraction process were approximately two to three times as large as those determined after the 24 h incubation process (Table 6). The phenol content was almost the same for railway sleepers and stakes that were treated or not treated with creosote under both conditions. It was thought that almost all of the water-extractable phenols determined in this study did not originate from the creosote-treatment but from phenol-structural compounds that were primarily contained in the wood or by the generation of oxidized compounds due to hydrolysis during the extraction process. The amount of phenols in the

Table 6
Content of water-extractable phenols in creosote-treated wood products

Sample	Creosote treatment	Water-extractable phenols (μg/g)	
		Autoclave (121 °C, 10 min)	Incubation (37 °C, 24 h)
1	Yes	706	319
2	Yes	363	181
3	Yes	392	176
4	Yes	533	50
5	Yes	360	74
6	No	425	113
7	Yes	324	158
8	No	529	193

creosote is also relatively low (Table 5), and the release of creosote from wood samples into water is minimal (Becker et al., 2001). Therefore, it is not important to measure water-extractable phenols in commercially-available wood samples.

4. Conclusion

This study demonstrated that varying amounts of PAHs and water-extractable phenols are present in creosote and creosote-treated wood products such as railway sleepers and stakes that are sold for agricultural purposes. Among carcinogenic PAHs, benz(*a*)anthracene was detected in the highest concentration, varying between 228 and 6328 μg/g in creosotes. Benzo(*b*)fluoranthene, benzo(*k*)fluoranthene and BaP were found in the range of 67–3541 μg/g. Almost all creosotes contained more than 50 μg/g of BaP, which is the upper limit level that is permitted in the EU standard. Creosote-impregnated wood products, such as brand-new or secondhand railway sleepers and foundations, also contained significant amounts of BaP (58–749 μg/g) and benz(*a*)anthracene (250–1282 μg/g). The concentration of phenols was low in creosotes and creosote-treated wood, and was not related to PAHs content. The effects of the water-extractable phenols on health might to be negligible. In Japan, creosotes containing a high concentration of BaP have been sold, and consumers are free to use them for wood preservation. This situation may cause impermissible health damage to persons handling creosotes and creosote-treated wood products, and the government has scheduled a restriction of the use of creosotes containing elevated amounts of carcinogenic PAHs.

References

Agency for Toxic Substances and Disease Registry (ATSDR), 2002. Toxicological profile for creosote, coal tar creosote, coal tar, coal tar pitch and coal tar pitch volatiles. US Department of Health and Human Services, Public Health Service, Atlanta, GA.

Anklam, E., Lipp, M., Müller, A., Van Eijk, J., Van Leemput, M., Van Steertegem, G., 1997. Results of collaborate trials concerning the analysis of benzo-*a*-pyrene in creosote. Fresenius J. Anal. Chem. 357, 1076–1080.

Becker, L., Matuschek, G., Lenoir, D., Kettrup, A., 2001. Leaching behaviour of wood treated with creosote. Chemosphere 42, 301–308.

Bestari, K.T.J., Robinson, R.D., Solomon, K.R., Steele, T.S., Day, K.E., Sibley, P.K., 1998. Distribution and composition of polycyclic aromatic hydrocarbons within experimental microcosms treated with creosote-impregnated Douglas fir pilings. Environ. Toxicol. Chem. 17, 2369–2377.

Commission of the European Communities, 2001. Commission Directive 2001/90/EC of 26th October 2001, adapting to technical progress for the seventh time Annex I to Council Directive 76/769/EEC on the approximation of the laws, regulations and administrative provisions of the Member States relating to restrictions on the marketing and use of certain dangerous substances and preparations (creosote). Official J. Eur. Communities L 283, 27/10/2001, pp. 41–43.

Commission of the European Communities, 2002. Commission Decision of 31 October 2002, concerning national provisions on restrictions on the marketing and use of creosote-treated wood notified by the Netherlands under Article 95(4) and (5) of the EU Treaty (2002/884/EC). Official J. Eur. Communities L 308, 9/11/2002, pp. 30–43.

Eriksson, M., Fldt, J., Dalhammar, G., Borg-Karlson, A.-K., 2001. Determination of hydrocarbons in old creosote-contaminated soil using headspace solid phase microextraction and GC–MS. Chemosphere 44, 1641–1648.

European Commission. Scientific Committee for Toxicity, Ecotoxicity and the Environment (CSTEE), 1999. Opinion (revised) on cancer risk to consumers from creosote containing less than 50 ppm benzo-[*a*]-pyrene and/or from wood treated with such creosote and estimation of respective magnitude expressed at the 8th CSTEE plenary meeting, Brussels, 4 March 1999.

Gevao, B., Jones, K.C., 1998. Kinetics and potential significance of polycyclic aromatic hydrocarbon desorption from creosote-treated wood. Environ. Sci. Technol. 32, 640–646.

International Agency for Research on Cancer (IARC), 1983. Polynuclear Aromatic Compounds, Part 1, Chemical, Environmental and Experimental Data, Summary of Data Reported and Evaluation. IARC Monographs 32, p. 211.

International Agency for Research on Cancer (IARC), 1987. Overall Evaluations of Carcinogenicity: An Updating of IARC Monographs Vols. 1–42, IARC Monographs, Suppl. 7, p. 177.

International Programme on Chemical Safety (IPCS), 1998. Selected Non-heterocyclic Polycyclic Aromatic Hydrocarbons. Environmental Health Criteria 202.

Japanese Industrial Standard (JIS), 2004. Wood Preservatives, JIS K 1570:2004.

Japan Wood Preserving Association (JWPA), online home page. http://wwwsoc.nii.ac.jp/jwpa/.

Journal of The Japan Aromatic Industry Association, Inc., online home page. http://www.jaia-aroma.com/.

Kohler, M., Künniger, T., Schmid, P., Gujer, E., Crockett, R., Wolfensberger, M., 2000. Iventory and emission factors of creosote, polycyclic aromatic hydrocarbons (PAH), and phenols from railroad ties treated with creosote. Environ. Sci. Technol. 34, 4766–4772.

Ou, S., Zheng, J., Zheng, J., Richardson, B.J., Lam, P.S., 2004. Petroleum hydrocarbons and polycyclic aromatic hydrocarbons in the surficial sediments of Xiamen Harbour and Yuan Dan Lake, China. Chemosphere 56, 107–112.

Pharmaceutical Society of Japan ed., 2000. Methods of Analysis in Health Science., Kanehara & Co., Ltd., Tokyo, p. 615.

Rotard, W., Mailahn, W., 1987. Gas chromatographic–mass spectrometric analysis of creosotes extracted from wooden sleepers installed in playgrounds. Anal. Chem. 59, 65–69.

Schwab, A.P., Su, J., Wetzel, S., Pekarek, S., Banks, M.K., 1999. Extraction of petroleum hydrocarbons from soil by

mechanical shaking. Environ. Sci. Technol. 33, 1940–1945.

Shu, Y.Y., Lai, T.L., Lin, H.-S., Yang, T.C., Chang, C.-P., 2003. Study of factors affecting on the extraction efficiency of polycyclic aromatic hydrocarbons from soils using open-vessel focused microwave-assisted extraction. Chemosphere 52, 1667–1676.

US Environmental Protection Agency (EPA), 1985. Evaluation and estimation of potential carcinogenic risks of polynuclear aromatic hydrocarbons. Carcinogen Assessment Group. Washington, DC.

US Environmental Protection Agency (EPA), 1993. Provisional Guidance for Quantitative Risk Assessment of Polycyclic Aromatic Hydrocarbons, EPA/600/R-93/089.

Woolgar, P.J., Jones, K.C., 1999. Studies on the dissolution of polycyclic aromatic hydrocarbons from contaminated materials using a novel dialysis tubing experimental method. Environ. Sci. Technol. 33, 2118–2126.

一般報文

ラット頭蓋冠由来骨芽細胞のALPase活性を促進する硫酸化ヒアルロン酸の効果

信州大学繊維学部　石黒（長幡）操・寺本　彰・阿部康次
国立医薬品食品衛生研究所療品部　中岡竜介・土屋利江

Enhancement action of sulfated hyaluronan on the ALPase activity of rat calvarial osteoblasts

Misao Nagahata-Ishiguro[*1,2], *Ryusuke Nakaoka*[*2], *Toshie Tsuchiya*[*2], *Akira Teramoto*[*1] *and Koji Abe*[*1]

[*1] Department of Functional Polymer Science, Faculty of Textile Science and Technology, Shinshu University, Ueda 386-8567, Japan
[*2] Division of Medical Devices, National Institute of Health Sciences, Tokyo 158-8501, Japan

Abstract : The purpose of this study was to clarify the effect of hyaluronan (Hya) and sulfated hyaluronan (SHya) on rat calvarial osteoblast (rOB) cells proliferation and differentiation *in vitro*. rOB cells were cultured in the presence of Hya with different molecular weights (0.2, 2, 30, 90, 120 x 10^4) for 10days. Hya did not affect the proliferation of rOB cells. However, SHya suppressed the proliferation of rOB cells. The alkaline phosphatase (ALPase) activity of rOB cells cultured with SHya for 10 days was significantly enhanced in comparison with control (in the absence of polysaccharides) and with Hya. Hya suppressed the ALPase activity of rOB cells. As a result, SHya can control rOB cells proliferation and differentiation. SHya suppressed the rOB cells proliferation in a few culture days and promoted the differentiation. It was suggested that these effects were based on the sulfate groups of SHya. Therefore, it is considered that SHya is useful for the biomedical material, which promotes the differentiation of rOB cells.

(Received 16 June, 2004; Accepted 20 December, 2004)

1. 緒　言

硫酸化多糖であるヘパリン（Heparin; Hep）やヘパラン硫酸（Heparan sulfate; HS）はheparin-binding growth factors（HBGFs）と複合体を形成し，組織が損傷を受けた場合，速やかにHBGFsを放出して，周辺の組織を活性化することが明らかとなっている[1-3]．HBGFsは，骨の修復にも重要な役割を果たしていることが知られ，骨芽細胞の増殖や分化の過程でオートクライン，パラクライン的に骨の形成や吸収を制御する[4-6]．病気やケガなどで骨組織が損傷した場合，修復するために人工骨や人工関節などの人工材料が用いられている．しかし，これらの人工材料は様々な問題があり，近年組織工学的手法を用いた骨再生が期待されている．この手法を用いて骨組織の再生に利用される細胞は，骨組織を形成する骨芽細胞である．骨芽細胞は間葉系由来の細胞で，未分化な間葉系の細胞から骨原性細胞を経て次第に成熟した骨芽細胞へと分化する．骨が大きく欠損した場合，細胞が増殖，分化するための足場が失われるため，仮の足場が必要となる．しかし，足場が優れていても細胞の数が少ないと十分な組織の再生は望めない．そこで、生体材料と増殖因子の組み合わせによる組織再生の方法が，近年多く報告されている[7, 8]．しかし，これらの増殖因子はたんぱく質であり，生体内での寿命が短く，不安定であるため，増殖因子を保持する担体が必要である．グリコサミノグリカンの構成成分であるヒアルロン酸（Hya）は，眼球、関節をはじめとする多くの結合組織に存在し，細胞外マトリックスの構成成分として，組織の創傷治癒や形態発生に重要な働きをしていることが報告されている[9-11]．近

年，Hyaのレセプターとして CD44 が発見されて以来，Hyaを介した生物学的機能の研究が盛んに行われている[12-14]．Pilloni らは，骨芽細胞の前駆細胞である間葉系細胞を用いて，分子量の異なるHyaの影響を検討しており[15]，Hyaは骨芽細胞の石灰化を促進すると報告している．しかし，細胞の増殖性，分化マーカーについての詳細な検討は行っていない．そこで本研究では，骨再生用材料の開発を目的として，生体適合性の高い多糖類を用いて骨組織の再生を試みた．本研究では、ヒアルロン酸と硫酸化多糖の機能を併せ持つ高分子量の硫酸化多糖を作製し，ラット頭蓋冠由来骨芽細胞[rat calvarial osteoblast（rOB cells）]の初期骨分化マーカーであるAlkaline phosphatase（ALPase）に対する影響について検討を行った．

2. 実験方法

2.1 材料

SHyaは以前に報告した方法にて合成した[16]．使用した硫酸化多糖の硫酸化度（D.S.；2糖残基当たり硫酸基の量）をTable 1に示した．HyaX(Xは分子量を示す)の分子量は0.2, 2, 30, 90, 120 x 10^4のもの使用した．Hya, SHya, コンドロイチン硫酸 typeC（Chs-C），Hepは0.5 mg/lの濃度になるように培地に溶解し，0.22 μmの孔径を有するfilterで滅菌をおこなった．HyaおよびSHyaの構造式をFig.1に示した．

Table 1 Characteristics of polysaccharides

Polysaccharides	Number of sulfate groups per two saccharide rings	MW (x10^4)
Hya	0	0.2-120
1.2SHya	1.2	55
2.1SHya	2.1	20
3.4SHya	3.4	5
Chs-C	1	0.5
Hep	2.5	1

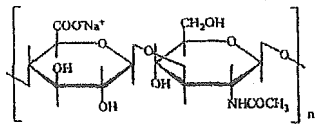

Hyaluronan (Hya)

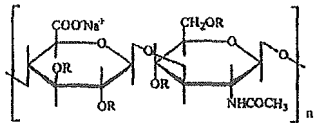

Sulfated hyaluronan (SHya)

R = $SO_3^-Na^+$ or H^+

Fig.1 Structure of hyaluronan and sulfated hyaluronan

2.2 細胞培養

生後48時間以内のウィスター系ラット（Charles River）の頭蓋冠から、酵素消化法により rOB cells を分離した[17]．その後，10% fetal bovine serum（FBS, GIBCO）を含むDulbecco's modified Eagle's medium（DMEM, Nissui-seiyaku）を用いて，初代培養を行った．3日毎に培地を交換しながら通常の継代培養を行い，継代数4-6の rOB cells を実験に使用した．

2.3 細胞増殖

多糖類と10% FBSを含むDMEMを用いて調製した rOB cells（1x10^4 cells/well, 24 multiwell plate）を播種し，5% CO_2下，37℃で培養した．所定時間培養後の細胞数を，下記のタンパク質量測定によって計測した．上澄みを除去し，well を phosphate-buffered salines（PBS; pH7.6）で3回洗浄した。0.04% nonidet P-40（NP-40, Nacalai tesque）を含む1ml PBSを各wellに添加し，37℃で10分間インキュベートした．懸濁液を超音波破砕機を用いてホモジナイズした後，1000rpm, 4℃, 5分間遠心を行った．この上澄液を細胞溶液として，Bio-Rad protein assay（protein assay, Bio-Rad Lab.）法により，595nm の吸光度を EIA READER を使って総タンパク質量を測定した．細胞数とタンパク質量の検量線を作成し，検量線により総タンパク質量から細胞数を算出した．検量線の作成法を以下に示す．0, 1, 5, 10, 30x10^5 cells/ml に調製した細胞懸濁液を各試験管に入れ，1000rpm, 4℃, 5分間遠心を行った．上澄みを除去し，0.04% NP-40を含む1ml PBSを各試験管に入れ，総タンパク質量を求め，細胞数と総タンパク質量の検量線を作成した．

2.4 Alkaline phosphatase（ALPase）活性

ALPase活性の測定は以下のようにして行った．細胞増殖の測定時に得られた細胞溶解液0.1mlと基質水溶液0.4ml（16mM p-nitrophenylphosphate disodium salt hexahydrate）を混合して，30分間，37℃でインキュベートした．その後，反応を停止するため，混合液に0.2N NaOH水溶液を0.5ml添加し，410nmの吸光度をEIA READERを用いて測定した．総タンパク量はBio-Rad protein assayによって測定し，Albumin(Bovine Albumin Fraction V）の検量線から算出した．

全ての実験において，実験数n=6として測定を行い，その平均値を求めた。

3. 結果

分子量の異なるHyaを添加した rOB cells の増殖曲線を，Fig.2に示した．培養7日目までは，Hyaの分子量に関係なく rOB cells は増殖し，コンフルエントに達した．しかし，培養10日目になると，高分子量のHyaを添加した rOB cells において，わずかに細胞数の増加が示され

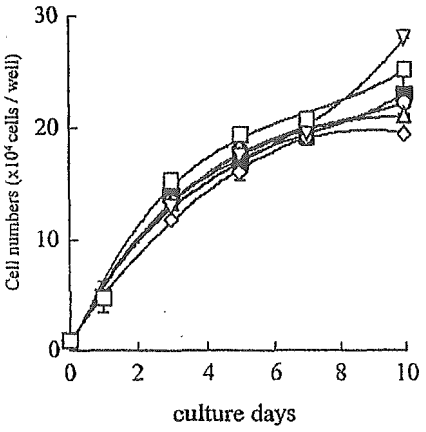

Fig.2 Effect of 0.5mg/ml hyaluronan on the proliferation of rOB cells

■ none ○ Hya0.2 △ Hya2 ◇ Hya30 ▽ Hya90 □ Hya120

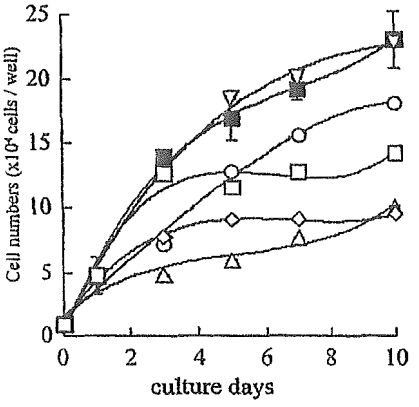

Fig.3 Effect of 0.5mg/ml sulfated polysaccharides on the proliferation of rOB cells

■ none ○ 1.2SHya △ 2.1SHya ◇ 3.4SHya ▽ Chs-C □ Hep

た.

Fig.3に，硫酸化度の異なるSHyaを添加したrOB cellsの増殖曲線を示した．Hyaを添加した場合と異なり，SHyaを添加したrOB cellsは，培養3日目から非添加系に比べて増殖が抑制された．さらに，SHyaの硫酸基の導入率が高くなるほど，rOB cellsの増殖は抑制された．これに対し，同じ硫酸基を有する多糖類であってもChs-Cではほとんど影響は見られず，Hepでも抑制効果は小さかった．

Fig.4に，Hyaを添加したrOB cellsのアルカリフォスファターゼ(ALPase)活性の経時変化を示した．Hyaは分子量に関係無く，骨芽細胞の初期分化マーカーであるALPaseの活性は非添加系に比べて低い値を示した．Fig.5に、硫酸化度の異なるSHyaを添加したrOB cellsのALPase活性を示した．Hyaとは異なり，SHyaを添加したrOB cellsのALPase活性は非添加系に比べて上昇が認められた．特に、高硫酸化度になるほど，ALPase活性の

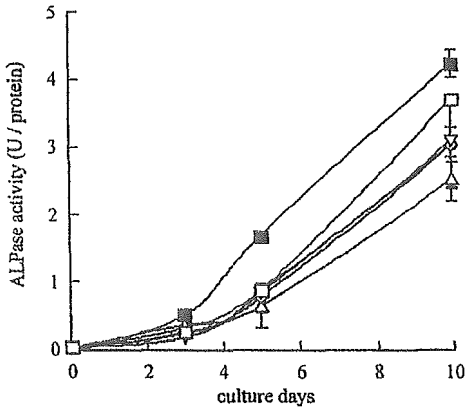

Fig.4 Effect of 0.5mg/ml hyaluronan on the ALPase activity of rOB cells

■ none ○ Hya0.2 △ Hya2 ◇ Hya30 ▽ Hya90 □ Hya120

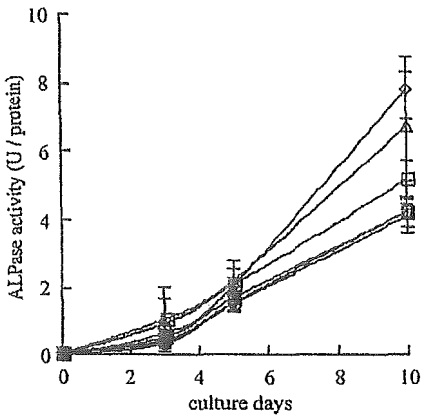

Fig.5 Effect of 0.5mg/ml sulfated polysaccharides on the ALPase activity of rOB cells

■ none ○ 1.2SHya △ 2.1SHya ◇ 3.4SHya ▽ Chs-C □ Hep

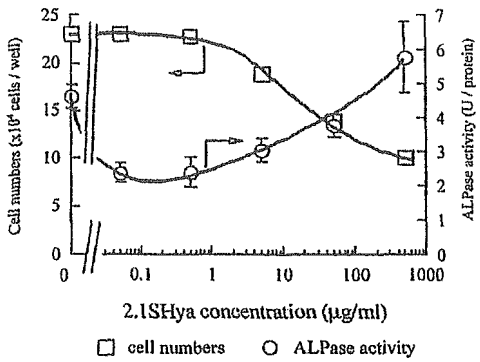

Fig.6 Dose-dependence of 2.1SHya on the proliferation and ALPase activity of rOB cells after 10days

上昇率は高かった．そこで，rOB cells の増殖と ALPase 活性に対する 2.1SHya の添加濃度の影響を検討した (Fig.6)．高濃度の SHya は rOB cells の増殖を抑制し，ALPase 活性を促進させたのに対し，低濃度の SHya は増殖を促進し，ALPase 活性を抑制させることが認められた．

4. 考察

本実験で我々は，分子量の異なる Hya を骨芽細胞に添加し，骨芽細胞の増殖と ALPase 活性について検討を行った．分子量 2000 から 120 万の Hya を rOB cells に添加したところ 非添加系とほとんど変わりなく増殖し，Hya 添加やその分子量の違いによる影響は見られなかった (Fig.2)．しかし，ALPase の活性は分子量に関係なく非添加系に比べてすべて低いため (Fig.4)，Hya は rOB cells の分化を抑制することが示唆された．Hep, HS は細胞外あるいは細胞表面に広く存在し，多くの種類のタンパク質と特異的な相互作用を示すことが知られている[18]．特に，ヘパラン硫酸プロテオグリカン (HSPG) は，細胞と ECM の相互作用や細胞同士の相互作用を介して，接着，凝集，シグナル伝達などに関与している．このように，多岐にわたる HSPG の機能の中で，増殖因子との相互作用については多くの報告があり，注目されている[1-3]．FGF, transforming growth factor-β(TGF-β), bone morphogenetic protein(BMP)などの細胞増殖因子は，Hep や HS などの硫酸化多糖と相互作用し，細胞の増殖を制御することが報告されている[1,4]．Hep, HS, Chs の分子量は，Hya に比べて非常に小さい．そこで本研究では，高分子量である SHya の骨再生用材料への応用を目的として，SHya 単独での rOB cells に対する影響を検討した．SHya の硫酸化度が高くなるにつれ，細胞の増殖は抑制され，Hep もある程度の抑制効果を示した(Fig.3)．ALPase 活性に対しては，硫酸化度が高くなるにつれて活性が上昇した(Fig.5)．これより，硫酸化多糖は細胞の増殖を抑制し，分化を促進させることが示された．次に，影響が最も大きく現れた 2.1SHya を用いて，濃度依存性について検討を行った．Fig.6 より，2.1SHya は低濃度では細胞の増殖を促進し，高濃度になるにつれ増殖を抑制した．これに対して ALPase 活性は低濃度では活性が低く，高濃度になるにつれ上昇した．これより，2.1SHya は濃度を変化させることで，rOB cells の機能を制御することが可能であることが示された．Hep, HS と増殖因子との協同的な作用の細胞の増殖に対する影響も，濃度によって大きく異なることが報告されている．Blanquaert らは，Hep 及び硫酸化多糖の RGTA(Heparin-like polymers derived from dextran)と増殖因子との協同作用による，マウス頭蓋冠由来骨芽細胞 MC3T3-E1 への影響を報告している[1]．RGTA は増殖因子と共に用いることで，増殖に対しては抑制的に働き，ALPase の活性が上昇することを明らかにした．この作用は RGTA のみでも影響が現れるが，増殖因子が存在することにより，さらに顕著に影響が現れた．今回，我々は SHya 単独の影響を検討したが，彼らの結果と一致する結果が得られた．以上の結果から，Hya に硫酸基を導入することにより，SHya は骨芽細胞の増殖や分化機能を制御することが可能であると示された．

5. 結論

rOB cells に Hya を添加すると，rOB cells の増殖は促進され，分化は抑制された．しかし，SHya を添加すると，rOB cells の増殖は抑制され，分化の促進が示された．SHya の効果は SHya の硫酸化度，濃度に大きく依存した．従って，SHya は骨芽細胞の機能を制御することが明かとなった．骨形成促進作用を持っている BMP, FGF2, TGF-β などの増殖因子を臨床応用に用いる場合，これらの増殖因子に適した担体の開発が必要である．SHya は分子量が高く，粘性があるため，増殖因子を保持する能力は Hep、HS などの他の硫酸化多糖に比べて高いことが考えられる．今後，SHya と増殖因子との相互作用について検討を行うことにより，SHya の分化促進作用の機序を明らかにできると同時に，SHya の骨再生用材料への応用が期待される．

6. 謝辞

本研究の一部は，21 世紀 COE プログラム，科学研究費補助金基盤研究(B)(14350495)，創薬等ヒューマンサイエンス総合研究事業，厚生労働科学研究費補助金（萌芽的先端医療技術推進研究，医薬品・医療機器等レギュラトリーサイエンス総合研究事業）の助成金により行われた．

文献

1. F. Blanuaert, D. Barritault and J. P. Caruelle, J. Biomed. Mater. Res., 44, 63 (1999)
2. E. Ruoslahti and D. Yamaguchi, Cell, 64, 867 (1991)
3. O. Saksela, D. Moscatelli, A. Sommer and D.B. Rifkin, J. Cel.l Biol., 107, 743 (1988)
4. D. J. Baylink, R. D. Finkelman and S. E. Mohan, J. Bone Miner. Res., 8, S565 (1993)
5. W. T. Bourque, M. Gross and B. K. Hall, Int. J. Dev. Biol., 37, 573 (1993)
6. M. E. Joyce, S. Jingushi , S. P. Scully and M. E. Bolander, Preg. Clin. Biol. Res., 365, 391 (1991)
7. H. Ueda , L. Hong , M. Yamamoto, K. Shigeno, M. Inoue, T. Toba, M. Yoshitani, T. Nakamura, Y. Tabata and Y. Shimizu, Biomaterials, 23, 1003

(2002)
8. C. H. Tang, R. S. Yang, H. C. Liou and W. M. Fu, J. Biomed. Mater. Res., **63**, 577 (2002)
9. P. H. Weigel, V. C. Hascall and M. Tammi, J. Biol. Chem., **272**, 13997 (1997)
10. W. Zhang, C. E. Watson, C. Liu, K. J. Williams and V. P. Werth, Biochem. J., **349**, 91 (2000)
11. L. S. Liu, C. K. Ng, A. Y. Thompson, J. W. Poser and R. C. Spiro, J. Biomed. Mater. Res., **62**, 128 (2002)
12. L. Sherma, J. Sleeman, P. Herrlich and H. Ponta, Curr. Opin. Cell. Biol., **6**,726 (1994)
13. P. W. Kincade,Z. Zheng, S. Katoh and L. Hanson, Curr. Opin. Cell. Biol., **9**, 635 (1997)
14. J. Entwistle, C. L. Hall and E. A. Turley, J. Cell Biochem., **61**, 569 (1996)
15. A. Pilloni and G. W. Bernard, Cell Tissue. Res., **294**, 323 (1998)
16. M. Nagahata, T. Tsuchiya, T. Ishiguro, N. Matsuda, Y. Nakatsuchi, A. Teramoto, A. Hachimori and K. Abe, Biochem. Biophys. Res. Commun.., **315**, 603-611 (2004)
17. T. Hamano, D. Chiba, K. Nakatsuka, M. Nagahata, A. Teramoto, Y. Kondo, A. Hachimori and K. Abe, Polym. Adv. Technol., **13**, 46 (2002)
18. E. Ruoslahti, Ann. Rev. Cell. Biol., **4**, 229 (1988)

ARTHRITIS & RHEUMATISM
Vol. 52, No. 1, January 2005, pp 155–163
DOI 10.1002/art.20713

Use of Bone Morphogenetic Protein 2 and Diffusion Chambers to Engineer Cartilage Tissue for the Repair of Defects in Articular Cartilage

Masashi Nawata,[1] Shigeyuki Wakitani,[1] Hiroyuki Nakaya,[2] Akira Tanigami,[3] Toyokazu Seki,[3] Yukio Nakamura,[1] Naoto Saito,[1] Kenji Sano,[1] Eiko Hidaka,[1] and Kunio Takaoka[4]

Objective. **To examine the ability of cartilage-like tissue, generated ectopically in a diffusion chamber using recombinant human bone morphogenetic protein 2 (rHuBMP-2), to repair cartilage defects in rats.**

Methods. **Muscle-derived mesenchymal cells were prepared by dissecting thigh muscles of 19-day postcoital rat embryos. Cells were propagated in vitro in monolayer culture for 10 days and packed within diffusion chambers (10^6/chamber) together with type I collagen (CI) and 0, 1, or 10 μg rHuBMP-2, and implanted into abdominal subfascial pockets of adult rats. Tissue pellets were harvested from the diffusion chambers at 2 days to 6 weeks after implantation, and examined by histology, by reverse transcription–polymerase chain reaction (PCR) for aggrecan, CII, CIX, CX, and CXI, MyoD1, and core binding factor a1/runt-related gene 2, and by real-time PCR for CII. Tissue pellets generated in the chamber 5 weeks after implantation were transplanted into a full-thickness cartilage defect made in the patellar groove of the same strain of adult rat.**

Results. **In the presence of 10 μg rHuBMP-2, muscle-derived mesenchymal cells expressed CII messenger RNA at 4 days after transplantation, and a mature cartilage mass was formed 5 weeks after transplantation in the diffusion chamber. Cartilage was not formed in the presence of 1 μg rHuBMP-2 or in the absence of rHuBMP-2. Defects receiving cartilage engineered with 10 μg rHuBMP-2 were repaired and restored to normal morphologic condition within 6 months after transplantation.**

Conclusion. **This method of tissue engineering for repair of articular defects may preclude the need to harvest cartilage tissue prior to mosaic arthroplasty or autologous chondrocyte implantation. Further studies in large animals will be necessary to validate this technique for application in clinical practice.**

Regeneration of articular cartilage is a challenging subject for research on joint surgery (1), and several methods have been devised and attempted in clinical practice to repair focal defects in articular cartilage, especially in young patients (2–5). Currently, mosaic arthroplasty (6), a procedure in which pieces of autogeneic chondro-osseous mass are procured from peripheral parts of the joint surface and transplanted into the focal cartilage defects, is often used with success in the knee joint (7). However, a number of limitations persist, and these include the limited source of the autogeneic osteochondral tissue mass and the potential risk of progression to osteoarthritis due to the injury caused by procurement of graft tissue from the normal joint surface. In addition, the functional durability of the repaired cartilage and the limited application of the approach to small joints are further areas of concern.

Recently, technologies have been developed in order to fabricate tissues for the repair of skeletal defects. The transplantation of chondrocytes of auto- or allogeneic origin has been demonstrated in both experimental (8–11) and clinical (12) situations. In these

Supported in part by a Grant-in-Aid for Scientific Research from the Japanese Ministry of Education, Culture, Sports, Science and Technology (16390436).

[1]Masashi Nawata, MD, Shigeyuki Wakitani, MD, PhD, Yukio Nakamura, MD, Naoto Saito, MD, PhD, Kenji Sano, PhD, Eiko Hidaka, PhD: Shinshu University School of Medicine, Matsumoto, Japan; [2]Hiroyuki Nakaya, MD: Osaka University Medical School, Osaka, Japan; [3]Akira Tanigami, MD, PhD, Toyokazu Seki, PhD: Otsuka Pharmaceutical Company, Tokushima, Japan; [4]Kunio Takaoka, MD, PhD: Osaka City University Medical School, Osaka, Japan.

Address correspondence and reprint requests to Shigeyuki Wakitani, MD, PhD, Department of Orthopaedic Surgery, Shinshu University School of Medicine, 3-1-1 Asahi, Matsumoto 390-8621, Japan. E-mail: wakitani@hsp.md.shinshu-u.ac.jp.

Submitted for publication May 6, 2004; accepted in revised form September 14, 2004.

cases, cells are dissociated from pieces of articular cartilage, propagated (or left unpropagated) on dishes in ex vivo conditions to expand the cell population, and then transplanted with or without scaffolding carrier materials into the cartilage defect of the recipient. Although these methods can repair cartilage defects, some difficulties persist. Allogeneic transplantation has the inherent risks of disease transmission and rejection; autologous transplantation causes damage to the donor site.

In an effort to address the limitations of existing approaches, we attempted to generate cartilage tissue by inducing the differentiation of muscle-derived cells into the chondrocytic lineage in an in vivo environment with recombinant human bone morphogenetic protein 2 (rHuBMP-2). Articular defects in rat joints that received the induced cartilage-like tissue were repaired and restored to normal condition. The present report provides evidence to support this approach for the successful treatment of articular cartilage defects.

MATERIALS AND METHODS

Preparation of muscle-derived mesenchymal cells and diffusion chambers. Mesenchymal cells were obtained from the thigh muscles of 19-day, postcoital, F344 rat embryos (purchased from Japan SLC, Hamamatsu, Japan). The muscle tissues were minced with scissors and digested in 0.25% trypsin with 1 m*M* EDTA-Na_4 (Invitrogen, Carlsbad, CA). The dissociated cells were propagated on plastic culture dishes (10 cm in diameter) in Dulbecco's modified Eagle's medium (Invitrogen) supplemented with 10% (volume/volume) fetal calf serum (Invitrogen) and antibiotics (mixture of 5 mg/ml penicillin G, 5 mg/ml streptomycin, 10 mg/ml neomycin; Invitrogen) and passaged under routine culture conditions for 10 days. At the end of this period, the cells were detached from the dishes with 0.25% trypsin with 1 m*M* EDTA-Na_4 and packed within diffusion chambers (10^6 cells/chamber).

In order to construct a diffusion chamber for cell transplantation, a diffusion chamber kit (Millipore, Billerica, MA), consisting of a plastic ring (14 mm in outer diameter and 10 mm in inner diameter), a membrane filter (comprising a mixture of cellulose acetate and cellulose nitrate [0.45 μm in pore size]), and adhesive sealant, was utilized. The inner diameter of the ring was reduced to 5 mm by inserting another plastic ring. Only one side of the larger plastic ring was initially sealed with a membrane filter and adhesive sealant. For the next step, 40 μl of 0.3% (weight/weight) pig type I collagen (Cellmatrix LA; Nitta Gelatin, Osaka, Japan) and 0, 1, or 10 μg of rHuBMP-2 (Yamanouchi Pharmaceutical, Tokyo, Japan) were introduced into the diffusion chamber. The chamber was then freeze-dried and sterilized with ethylene oxide gas.

After these processes were completed, 10^6 cells suspended in 40 μl of serum-free culture medium containing 0.3% (w/w) pig type I collagen (Cellmatrix I-A; Nitta Gelatin) were introduced into the diffusion chamber, and another open side of the chamber was sealed with a filter and adhesive sealant. Sixty-two chambers (42 for histologic examination, 8 for reverse transcription–polymerase chain reaction [RT-PCR] analysis, and 12 for real-time PCR analysis) with 10 μg of rHuBMP-2 (group B10), 10 chambers (all for histologic examination) with 1 μg of rHuBMP-2 (group B1), and 46 chambers (26 for histologic examination, 8 for RT-PCR analysis, and 12 for real-time PCR analysis) without rHuBMP-2 (group B0) were prepared for analysis and implantation.

Transplantation of the diffusion chamber into the abdominal pocket of rats. Immediately after loading the cells into the diffusion chambers, each chamber was surgically inserted into a pocket in the abdominal muscles of 8-week-old F344 rats under diethyl ether anesthesia. After surgery, the rats were housed in cages and were given free access to standard chalk-like food and water. At 2, 4, 6, 8, 14, 21, 28, 35, and 42 days after implantation, the animals were killed in due order and the diffusion chambers were harvested (Table 1) for histologic examination. For RT-PCR analysis, 2 chambers were harvested at 2-, 4-, 7-, and 14-day intervals after implantation. For real-time PCR analysis, 2 chambers were harvested at 2-, 4-, 6-, 14-, 28-, and 42-day intervals after implantation.

Harvested tissue pellets within the chambers were inspected for vascular invasion caused by seal failure or breakage of the filter membranes. When vascular invasion was noted, the tissue was excluded from the transplantation into the cartilage defect and from PCR analysis. The tissue pellets for histologic examination were radiographed and fixed in 20% neutral buffered formalin solution, prior to processing for histologic examination. Some parts of the tissue pellet from the 5-week-old sample were used for transplantation into the rat-knee defect. Tissue pellets for RT-PCR or real-time PCR were frozen in liquid nitrogen immediately after harvesting.

Transplantation of tissue pellets from diffusion chambers into osteochondral defects of rats. Some portions of the tissue pellet removed from the diffusion chambers at 5 weeks after implantation were transplanted into cartilage defects generated on the patellar grooves of the knee joints of 7 (4 from group B10, 3 from group B0) mature, same-strain rats (a quarter tissue pellet/animal). The transplantation procedure was performed with the rats under anesthesia, using an intramuscular injection of a mixture of ketamin (100 mg/ml, 0.6

Table 1. Cartilage formation in diffusion chamber*

	rHuBMP-2			Area of cartilage tissue in cross-section
	0 μg	1 μg	10 μg	
2 days	0/2	–	0/2	–
4 days	0/2	–	0/2	–
6 days	0/2	–	0/2	–
8 days	0/2	–	0/2	–
14 days	0/2	–	0/2	–
21 days	0/4	–	4/6	1/4
28 days	0/4	0/4	9/10	1/3
35 days	0/4	0/6	9/10	Almost all
42 days	0/4	–	6/6	Almost all

* Except where indicated otherwise, values are the number of samples with cartilage formation/number of experiments. rHuBMP-2 = recombinant human bone morphogenetic protein 2.

ml/kg body weight; Sankyo, Tokyo, Japan) and xylazine (20 mg/ml, 0.3 ml/kg body weight; Bayel, Osaka, Japan). Pellets were transplanted into the left knees, and defects made on the right knees did not receive the implants.

In order to generate an osteochondral defect on the patellar groove of the distal femur of the rats, a longitudinal skin incision was made in the midline of the knee and the patellar groove was exposed by medial parapatellar arthrotomy and lateral dislocation of the patella. The osteochondral defect was made by drilling in 2 mm in depth and 2 mm in diameter, vertically to the patellar groove. The tissue pellet was detached from the inner surface of the membrane filters of the diffusion chamber and press-fitted into the defect. The knee joint was then closed with sutures. After surgery, the rats were fed in cages and killed at 24 weeks after surgery. The knee joints were excised and processed for histologic examination.

Histologic examination. Diffusion chambers and distal femurs with an articular cartilage defect were removed from the animals at 24 weeks after implantation and fixed in 20% buffered formalin. The harvested chambers were radiographed with a soft x-ray apparatus (Sofron, Tokyo, Japan) and visualized on radiographic films (Fuji Photo Film, Tokyo, Japan). The harvested chambers with calcified tissue and the distal ends of femurs with articular defects were decalcified in 4% EDTA solution, and then dehydrated with a gradient ethanol series, embedded in paraffin, sectioned in 5-μm thickness, and stained with hematoxylin and eosin or toluidine blue. Results of the histologic examination were evaluated using the scoring system described by Wakitani et al (13) for histologic grading of a cartilage defect (Wakitani's score; a lower score indicates improvement).

RT-PCR analysis. In order to detect changes in the expression of cartilage matrix–specific molecules in cells from the harvested diffusion chambers, RT-PCR analyses for aggrecan, types II, IX, X, and XI collagens, MyoD1, and core binding factor a1 (Cbfa1)/runt-related gene 2 (Runx2) were performed with the tissue pellets from the B10 and B0 groups. Frozen tissue pellets were ground down to powder with liquid nitrogen in a mortar on dry ice, and total messenger RNA (mRNA) was extracted from the tissue using TRIzol reagent (Invitrogen) according to the manufacturer's instructions. After treating samples with RNase-free deoxyribonuclease I (Takara Bio, Otsu, Japan), 500 ng of total mRNA from each sample was reverse transcribed using SuperScript II (Invitrogen). The reaction time was 60 minutes at 42°C. Thereafter, 1 μl of each reaction product was amplified in a 15-μl PCR mixture containing 0.5 units TaKaRa EX Taq (Takara Bio) and 10 pmoles of each primer to detect mRNA specific to each molecule.

Amplifications were performed in a Program Temp Control System (DNA Engine PTC-200; MJ Research, Waltham, MA) for 35 cycles after an initial denaturation step at 95°C for 3 minutes, denaturation at 95°C for 30 seconds, annealing for 30 seconds at 60°C, and extension at 72°C for 30 seconds, with a final extension at 72°C for 3 minutes. The PCR products (10 μl) were electrophoresed in a 3% agarose gel and detected by ethidium bromide staining. The nucleotide sequences of the primers for each of these genes are as follows: for AGC1, 5′-TCCAAACCAACCCGACAAT-3′ (forward) and 5′-TTCTGCCCAAGGGTTCTG-3′ (reverse); for Col2A1, 5′-GCTCGAGGAGACACTGGTG-3′ (forward) and 5′-ACCTGGGGGACCATCAGA-3′ (reverse); for Col9A1, 5′-GGTCCTCCGGGGAAGCCT-3′ (forward) and 5′-CCAACCTCTCCCGGCGGT-3′ (reverse); for Col10A1, 5′-CGAGGTCTTGTTGGCCCTAC-3′ (forward) and 5′-CCTGGGTCTCTGTCCGCT-3′ (reverse); for Col11A1, 5′-ATTGCCACCAGTCAACTGCT-3′ (forward) and 5′-TTGGACTGTGCCTCCGTC-3′ (reverse); for MyoD1, 5′-ACTACAGCGGCGACTCAGAC-3′ (forward) and 5′-GTGGAGATGCGCTCCACTAT-3′ (reverse); and for Cbfa1/Runx2, 5′-TGCTTCATTCGCCTCACAAAC-3′ (forward) and 5′-TAGAACTTGTGCCCTCTGTTG-3′ (reverse).

Real-time quantitative RT-PCR. Quantitative RT-PCR assay for type II collagen was carried out with the use of gene-specific expression–labeled fluorescent probes and sets of specific primers in an ABI PRISM 7700 sequence detection system (Applied Biosystems, Foster City, CA). On the basis of the published sequence of rat type II collagen, specific primer pair and probe sets were designed with the aid of Primer Express software, version 2.0 (Applied Biosystems). The sequences of the primers were 5′-AGGCGCTTCTGGTAACCCA-3′ (forward) and 5′-GACCAGTTGCACCTTGAGGAC-3′ (reverse), and the probe was 5′-TTCCCGGAGCCAAAGGATCTGCTG-3′. We used 6-carboxyfluorescein for type II collagen as the 5′ fluorescent reporter for the probe, while we added 6-carboxy-tetramethylrhodamine (Tamura Pharmaceutical, Osaka, Japan) to the 3′ end as a quencher.

Standard curves were constructed with the use of dilutions of accurately determined pCR2.1 plasmid vector (Invitrogen) containing complementary DNA (cDNA) products of type II collagen. A relative standard curve representing 10-fold dilutions of a rat type II collagen cDNA ranging from 2×10 to 2×10^5 copies/μl was used for linear regression analysis of the samples. PCR was carried out in 50 μl of reaction mixture containing 3 μl of the RT reaction, 1× Universal Master Mixture (Applied Biosystems), 500 n*M* of each primer, and 200 n*M* of the Taqman probe purchased from Applied Biosystems.

To compensate for the differences in cell number and/or RNA recovery, the copy number of type II collagen mRNA was determined relative to 18S ribosomal RNA (rRNA) (Applied Biosystems), which was also analyzed quantitatively. Thus, a partial cDNA of 18S rRNA was amplified from rat bone and cartilage samples using a specific primer set for 18S rRNA, and then subcloned into pCR2.1 (Invitrogen). Ten-fold dilutions of the resultant vector, pCR2.1-18S rRNA, ranging from 2×10 to 2×10^5 copies/μl, were used to construct a relative standard curve for 18S rRNA. The PCR mixture was basically the same as that for type II collagen, except for 200 n*M* of an 18S rRNA–specific Taqman probe set carrying a 5′-VIC reporter label and 3′-TAMURA quencher group, and 500 n*M* of the specific primer for 18S rRNA that was purchased from Applied Biosystems. These samples were placed in the ABI PRISM 7700 Sequence Analyzer and preheated at 95°C for 10 minutes, then amplified for 50 cycles of 95°C for 15 seconds, followed by 60°C for 1 minute. These experimental protocols were in compliance with the guidelines established by the Institutional Committee for Animal Care and Experiments of Shinshu University.

Statistical analysis. The histologic score was statistically analyzed using the SPSS software package (SPSS Japan, Tokyo, Japan). The Kruskal-Wallis H test followed by the

Mann-Whitney U test was used to determine differences between the groups.

RESULTS

Cartilage induction in diffusion chambers by rHuBMP-2. The tissue mass harvested from group B10 chambers (those receiving 10 μg rHuBMP-2) had a gelatinous appearance, with no histologic features characteristic of cartilage until 2 weeks after implantation. At 3 and 4 weeks after implantation, the tissue had a pale, opaque gelatinous appearance and revealed some cartilaginous characteristics along the inner surface of the filter membranes of the chamber on histologic examination (Figures 1A–H).

At 5 and 6 weeks postimplantation (Figures 1I–P), the cells of group B10 formed an elastic tissue mass with opaque appearance and no evidence of calcification on radiography (Figure 2B). Histologic examination of the opaque tissue mass in the chambers indicated normal features of cartilage, with round chondrocytic cells enclosed in a metachromatic matrix, as revealed by toluidine blue staining (Figures 1L and P). Small amounts of osseous tissue were found on the outer or host-side surfaces of the membrane filter of those samples. In one chamber with an accidental "hole" on the membrane filter, containing 5-week postimplantation tissue of group B10, the tissue became a hard mass with a reddish appearance; on radiography, the tissue was highly calcified (Figure 2C) and showed a normal histologic appearance of bone with hematopoietic marrow (Figure 2A). In contrast, the tissue of groups B0 (Figure 1) and B1 (chambers without rHuBMP-2 or with 1 μg rHuBMP-2, respectively) showed a gelatinous appearance with no histologic evidence of cartilage formation throughout the experimental period.

PCR findings. PCR analysis of the tissue in the diffusion chambers revealed a consistent expression of types X and XI collagen (Figure 3). Expression of type X collagen gradually increased in group B10. The expression of type II collagen was detected at low levels 2 days after implantation in group B10 (Figure 3). After 4 days, the expression of type II collagen was clearly detected in group B10. The expression of Cbfa1/Runx2 was clearly detected after 96

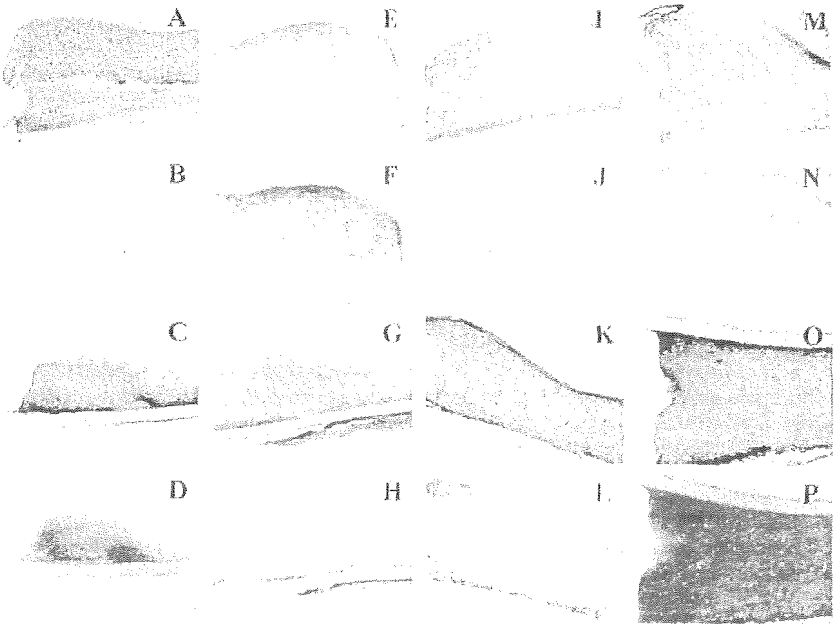

Figure 1. Cartilage formation in the diffusion chamber. Tissue pellets in diffusion chambers were examined at 3 weeks (A–D), 4 weeks (E–H), 5 weeks (I–L), and 6 weeks (M–P) postimplantation, in group B0 (without recombinant human bone morphogenetic protein 2 [rHuBMP 2]) (A, B, E, F, I, J, M, and N) compared with group B10 (with 10 μg rHuBMP 2) (C, D, G, H, K, L, O, and P). (Stained with hematoxylin and eosin in A, C, E, G, I, K, M, and O, with toluidine blue in B, D, F, H, J, L, N, and P; original magnification × 40.)

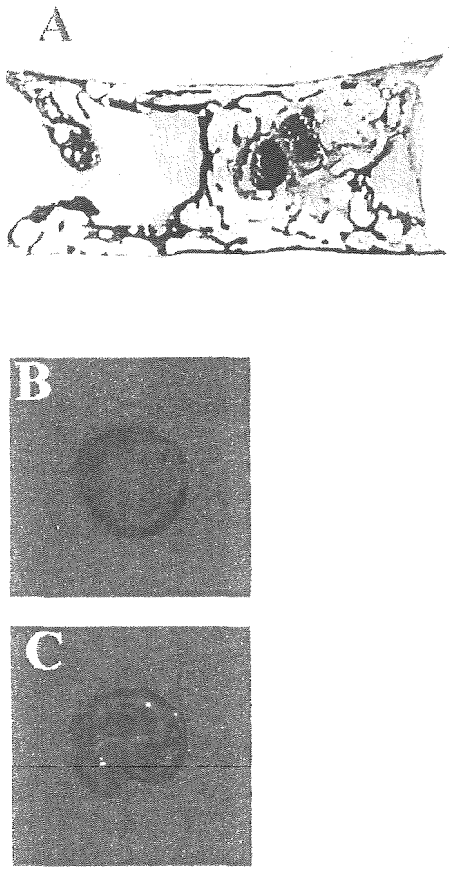

Figure 2. Histologic and radiologic evaluations of engineered cartilage tissue. For the tissue pellet in the diffusion chamber with an accidental hole on the filter (at 5 weeks posttransplantation; obtained from group B10), the normal histologic appearance of bone is clearly visible (stained with hematoxylin and eosin; original magnification ×20) (A), and the soft radiographic view shows bone trabeculae (C). Another soft radiographic view of group B10 tissue (same sample as in Figures 1K and 1L) shows no calcification (B).

hours in group B10 only (Figure 3). The expression of MyoD1 was not detected in either group at any time point.

Real-time PCR revealed that the expression of type II collagen increased markedly at 4 days after implantation (Figure 4). A high level of aggrecan was seen in group B10 after 2 days. Type IX collagen was weakly expressed in group B10 after 4 days, but increased significantly after 1 week. Low expression levels of aggrecan and type II collagen were detected in all groups at later time points in the study.

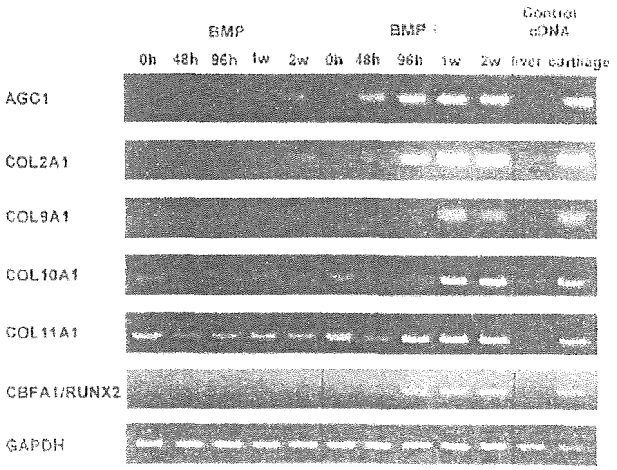

Figure 3. Reverse transcription–polymerase chain reaction analysis. Expression of types X and XI collagen (COL10A1 and COL11A1, respectively) was detected consistently in both groups (with 10 μg recombinant human bone morphogenetic protein 2 [BMP +]: group B10] and without [BMP −]) throughout the experimental period. Expression of type IX collagen (COL9A1) was detected after 96 hours, indicating that effective cartilage matrix synthesis begins 3 or 4 days after implantation. Expression of type II collagen (COL2A1) was detected at low levels after 2 days in group B10 only, and after 4 days, it became more prominent. The expression of core binding factor a1/runt-related gene 2 (CBFA1/RUNX2) was clearly detected after 96 hours in group B10 only. AGC1 = aggrecan.

Repair of cartilage defects by transplantation of the engineered cartilage. The osteochondral defects that received the cartilaginous tissue mass, which was generated for 5 weeks in diffusion chambers containing tissue from group B10, were restored to a normal appearance at 24 weeks after transplantation. Upon examination, the site of the defects had a smooth surface and no

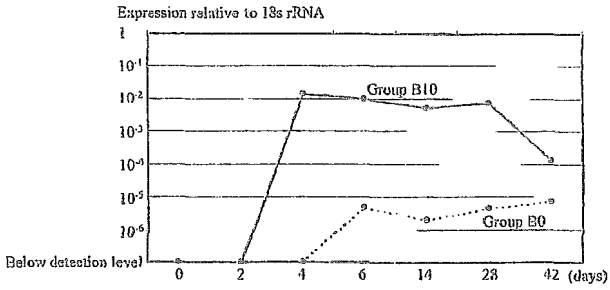

Figure 4. Real-time polymerase chain reaction analysis for type II collagen mRNA. After 4 days, expression of type II collagen mRNA was markedly increased in group B10 (with 10 μg recombinant human bone morphogenetic protein 2 [rHuBMP 2]). Group B0 = without rHuBMP 2; rRNA = ribosomal RNA.

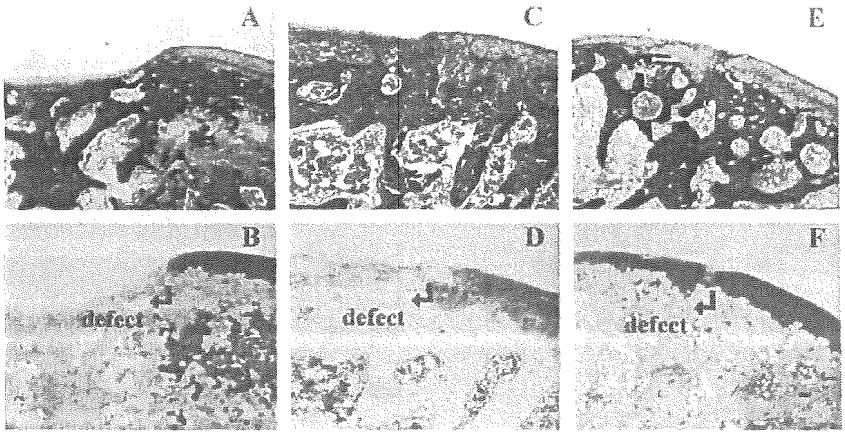

Figure 5. Osteochondral defects of a rat knee repaired with tissue pellets generated in diffusion chambers 24 weeks after transplantation. A and B, Defect with no implant. C and D, Defect implanted with tissue pellet generated in the chamber of group B0 (without recombinant human bone morphogenetic protein 2 [rHuBMP 2]). E and F, Defect implanted with tissue pellet generated in the chamber of group B10 (10 μg rHuBMP-2). (Stained with hematoxylin and eosin in A, C, and E, with toluidine blue in B, D, and F; original magnification × 40.)

obvious border with the surrounding normal articular cartilage (Figures 5E and F). The defects were filled with a layer of cartilage exhibiting subchondral cancellous bone connecting to the original subchondral bone. Although the architecture of the repaired articular cartilage was similar to that of normal cartilage with regard to cell arrangement, differences were noted. A tidemark was visible at the base of the cartilage layer adjacent to the subchondral bone, and the thickness of the regenerated cartilage was slightly less than that of the neighboring normal articular cartilage.

In contrast, the defects transplanted with tissue mass from group B0 were partially repaired, with a depressed surface visible at the defect site (Figures 5C and D). Histologic assessment of the defects that received either the tissue from group B0 or no implant revealed a small amount of fibrocartilage, with slightly positive metachromatic staining at the periphery of the defects and dominant fibrous tissue in the defect space.

Upon histologic evaluation of the knee cartilage after repair, the average histologic score (Wakitani's score) was 4.25 for group B10, 11.67 for group B0, and 14.00 for the defect-only group. The score for group B10 was significantly better than that for group B0 ($P = 0.032$) and the defect-only group ($P = 0.002$).

DISCUSSION

The experimental data presented herein indicate the capacity of rHuBMP-2 to induce the differentiation of young muscle-derived mesenchymal cells into chondrocytes within diffusion chambers in in vivo conditions. The resultant heterotopic cartilage formation represents a significant volume of induced tissue mass derived from these cells.

In order to induce the cartilage tissue, the diffusion chamber system was essential. When vascular invasion into the chamber occurred as a result of membrane seal failure, new bone with hematopoietic marrow was seen in the chambers harvested at 5 weeks after transplantation. Budenz and Bernard have reported similar findings (14). This bone was likely formed through the process of endochondral ossification, as deduced from classic reports describing the actions of BMP (15) and from comparison with the process of direct ossification (16,17). In the process of BMP-induced endochondral bone formation, cartilage is formed in the early phase of the bone-forming process. The cartilage tissue is then absorbed by invading vascular connective tissue and replaced by newly formed bone, as seen in embryonic osteogenesis (18) and in callus in fracture repair (19). During the process of ectopic bone formation elicited by